Acta Crystallographica Section F
Structural Biology and Crystallization Communications
ISSN 1744-3091

Cloning, expression, purification and preliminary crystallographic analysis of the short-chain dehydrogenase enzymes WbmF, WbmG and WbmH from *Bordetella bronchiseptica*

Nicholas J. Harmer,[a]*‡ Jerry D. King,[a,b]§ Colin M. Palmer,[a] Andrew Preston,[b,c]¶ Duncan J. Maskell[b] and Tom L. Blundell[a]

[a]Department of Biochemistry, 80 Tennis Court Road, Cambridge CB2 1GA, England, [b]Department of Veterinary Medicine, Cambridge CB3 0ES, England, and [c]Department of Molecular and Cellular Biology, University of Guelph, Ontario N1G 2W1, Canada

‡ Current address: AstraZeneca R&D Mölndal, 431 83 Mölndal, Sweden.
§ Current address: Department of Molecular and Cellular Biology, University of Guelph, Ontario N1G 2W1, Canada.
¶ Current address: Department of Clinical Veterinary Science, University of Bristol, Langford House, Langford BS40 5DU, England.

Correspondence e-mail: nic@cryst.bioc.cam.ac.uk

Received 6 June 2007
Accepted 17 July 2007

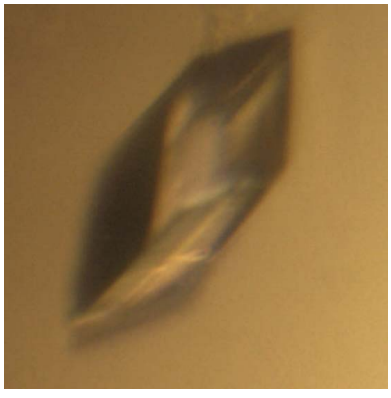

The short-chain dehydrogenase enzymes WbmF, WbmG and WbmH from *Bordetella bronchiseptica* were cloned into *Escherichia coli* expression vectors, overexpressed and purified to homogeneity. Crystals of all three wild-type enzymes were obtained using vapour-diffusion crystallization with high-molecular-weight PEGs as a primary precipitant at alkaline pH. Some of the crystallization conditions permitted the soaking of crystals with cofactors and nucleotides or nucleotide sugars, which are possible substrate compounds, and further conditions provided co-complexes of two of the proteins with these compounds. The crystals diffracted to resolutions of between 1.50 and 2.40 Å at synchrotron X-ray sources. The synchrotron data obtained were sufficient to determine eight structures of the three enzymes in complex with a variety of cofactors and substrate molecules.

1. Introduction

The *Bordetella* species *B. parapertussis* and *B. bronchiseptica* are widely studied pathogens that infect the respiratory tracts of mammals. *B. parapertussis* is associated with approximately 5% of cases of whooping cough in humans (Cherry, 1996) and a separate lineage causes respiratory infections in sheep (Porter *et al.*, 1994). *B. bronchiseptica* has a broad host range and is a cause of kennel cough (Burns *et al.*, 1993) and atrophic rhinitis (Magyar *et al.*, 1988) in dogs and pigs, respectively. Lipopolysaccharide (LPS), the major component of the outer leaflet of the outer membrane, is one of the virulence factors implicated in infections by these bacteria. *B. parapertussis* and *B. bronchiseptica* are closely related and LPS in both species is substituted with an O antigen, which elicits a strong immunological response in infected animals and protects against complement-mediated killing *in vitro* (Burns *et al.*, 2003).

The synthesis of the O antigen has been localized to a single genetic locus in these bacteria, the *wbm* locus (Preston *et al.*, 1999). This locus contains 24 genes, many of which are similar to the O-antigen synthesis genes described in other bacteria. Based on the homology of the genes in the *wbm* locus to proteins of known function and on the activities required to produce the sugar residues found in the mature O antigen, we have devised a path to the synthesis of each component of this structure and are in the process of verifying various steps (JDK, AP and DJM, unpublished observations). However, some of the steps cannot be unambiguously assigned to a single gene product. In particular, genome sequencing has revealed that the *wbm* locus contains three neighbouring genes (*wbmF*, *wbmG* and *wbmH*) with homology to the widespread short-chain dehydrogenase/reductase (SDR) gene family that are proposed to carry out the epimerization of UDP-ManNAcNAcAN at the 3′ and 5′ positions. This reaction requires three distinct activities (4′-oxidation, 3′,5′-epimerization and 4′-reduction). All of these activities can be carried out by SDR enzymes and indeed a single enzyme capable of catalysing all three activities with an analogous sugar-nucleotide substrate has been described (Major *et al.*, 2005). However, there are many examples where multiple enzymes are

required to carry out the 3′,5′-epimerization (Ginsburg, 1960, 1961; Tonetti *et al.*, 1998; Giraud & Naismith, 2000).

Genetic studies of *wbmF*, *wbmG* and *wbmH* have supported a role for each of these genes in synthesis of the O antigen (King *et al.*, 2007), but could not distinguish unambiguous roles for any one of the encoded enzymes. In addition, since SDR enzymes tend to have low sequence identities to one another (typically 15–30% identity to the nearest non-orthologue), it is not possible to predict the likely activity of these enzymes from their sequences.

Structural analysis of these enzymes should allow the identification of the amino acids that are associated with the active site in each enzyme and provide a clearer view of the probable catalytic activities of each. In addition to unravelling the molecular basis of the synthesis of the O antigen in these pathogens, the structural analysis should also prove a test of the idea that structural studies can be used to determine the function of proteins of known class but unknown activity.

2. Cloning, expression and purification of WbmF, WbmG and WbmH

The full-length coding sequences of WbmF (GeneID 2660132), WbmG (GeneID 2662020) and WbmH (GeneID 2660170) were inserted into pET15b (Novagen) using the *Nde*I (NEB) and *Bam*HI restriction sites. *B. bronchiseptica* chromosomal DNA was prepared by suspending a single bacterial colony in 500 µl water and incubating in boiling water for 5 min. The resulting suspension was centrifuged at 14 500*g* for 2 min and the supernatant was used as a template for the PCR reaction. PCR primers were designed to introduce an *Nde*I site including the native start codon and a *Bgl*II site after the stop codon. The resulting expression constructs contain a 6×His tag, a thrombin cleavage site and the full-length coding sequence of the relevant enzyme. The 6×His tag was not removed during purification, resulting in an N-terminal cloning artefact sequence of MGSSH-HHHHHSSGLVPRGSH in all three proteins. Including these residues, the final constructs encoded proteins that contained 377, 330 and 333 amino acids and had expected molecular weights of 41 536, 35 247 and 36 586 Da for WbmF, WbmG and WbmH, respectively.

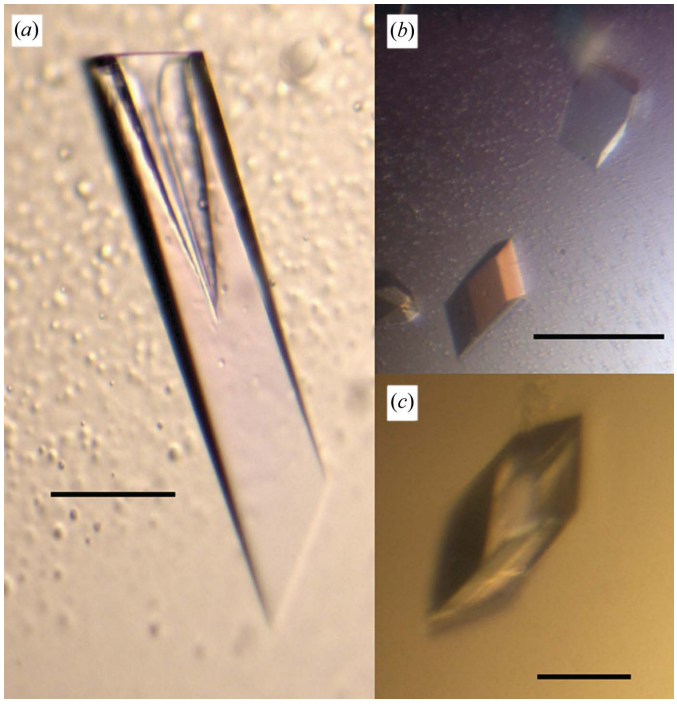

Figure 1
Representative crystals of WbmF, WbmG and WbmH: representative crystals of the major crystal forms used in this study are shown. (*a*) Crystal of WbmF after approximately 10 d growth. The conic hollows in the crystals were characteristic of this crystal from. (*b*) Crystals of WbmG after approximately 12 d growth. (*c*) The one diffraction-quality crystal of WbmH that was grown, pictured at the end of its growth. The scale bar corresponds to 100 µm in (*a*) and (*b*) and 10 µm in (*c*).

The expression constructs were transformed into BL21 (DE3) cells (Novagen) and grown in 2×YT medium supplemented with 100 µg ml^{-1} carbenicillin at 310 K. When the optical density of the medium at 600 nm reached 0.5, expression of the protein was induced by the addition of 0.4 m*M* IPTG and the cells were grown for 5 h at 288 K. The cells were harvested by centrifugation and resuspended in 25 ml resuspension buffer (20 m*M* Tris–HCl pH 8.0, 0.5 *M* NaCl supplemented with one tablet per 50 ml of Complete EDTA-free protease inhibitors; Roche) per litre of culture.

The bacterial cells were lysed by sonication (XL sonicator, Misonix) and clarified by centrifugation at 21 000*g* for 20 min, followed by 0.22 µm filtration of the supernatant. WbmF, WbmG and WbmH were purified by nickel-affinity chromatography using a 1 ml HisTrap HP column (GE Healthcare): the column was equilibrated in lysis buffer (without protease inhibitors) and charged with clarified lysate (from 1 l expression volume). Following binding, the column was washed thoroughly with 20 m*M* Tris–HCl pH 8.0, 0.5 *M* NaCl, 5 m*M* imidazole and the target protein was eluted using a gradient to 125 m*M* imidazole over 20 column volumes. Following this, the protein was purified by size-exclusion chromatography using a Superdex 75 26/60 column (GE Healthcare) with an elution buffer of 20 m*M* Tris–HCl pH 8.0, 150 m*M* NaCl and a flow rate of 1 ml min^{-1}. The typical yield from 1 l expression was 35 mg purified protein. The purified protein was then concentrated using VivaSpin columns (Vivascience) with a molecular-weight cutoff of 10 kDa to an appropriate concentration in the size-exclusion elution buffer. The protein was subsequently crystallized in this buffer. In the case of WbmF, the chromatography steps were both completed within 8 h of cell lysis; NAD^+ or NADH was added to the sample to a concentration of 1 m*M* immediately following elution from the size-exclusion chromatography column and the protein was concentrated with cofactor present. These steps significantly improved the yield and stability of the purified protein and crystallization was not successful using material to which cofactor had not been added.

Selenomethionine-labelled WbmG was prepared using the method of Van Duyne *et al.* (1993). The yield was slightly lower than that of nonlabelled material. Mass spectrometry indicated that the extent of labelling was >95% (data not shown).

3. Crystallization of WbmF, WbmG and WbmH

Initial crystallization screening of each protein and of cocrystals of WbmF and WbmG with UDP was carried out using sitting-drop vapour diffusion at 293 K. Each protein was screened using mother liquors from Crystal Screens 1 and 2 (Hampton Research) and from either the Wizard I and II crystallization screens (Emerald Biostructures; protein with cofactors) or from the broadly equivalent SM1 screen (Qiagen; protein–UDP cocrystals). For each crystallization condition, 100 µl mother liquor was added to a reservoir in a 96-well CrystalQuick crystallization plate with square sitting-drop positions (Molecular Dimensions). Three sitting drops were established in the shelves adjacent to the reservoir using a Honeybee 81 crystallization robot (Genomic Solutions). Each sitting drop

contained 100 nl mother liquor and 100 nl protein solution. A separate plate was used for each protein; each experiment tested two concentrations of each protein (7 and 14 mg ml^{-1} for WbmF, 8 and 16 mg ml^{-1} for WbmG and 5 and 10 mg ml^{-1} for WbmH), with a buffer control in the third position. Conditions that yielded crystals were optimized with manually prepared conditions using 24-well Linbro plates and glass cover slides (Hampton Research).

Diffraction-quality crystals of WbmF were optimized from Wizard I conditions 1 and 21 and the Wizard II conditions 3 and 24. Crystals (in complex with NAD^+ or NADH) were grown using hanging-drop vapour diffusion at 293 K over a 500 µl reservoir containing 16%(*w*/*w*) PEG 8000, 0.1 *M* Bicine pH 9.0. Each drop contained 2 µl WbmF at 14 mg ml^{-1}, with NAD^+ or NADH at 1 m*M* and 2 µl mother liquor. Diffraction-quality crystals grew in 3 d, reaching dimensions of 0.3 × 0.1 × 0.1 mm (Fig. 1*a*).

Diffraction-quality crystals of WbmG were optimized from Wizard II condition 3. Crystals were grown using hanging-drop vapour diffusion at 293 K over a 500 µl reservoir containing 16–18%(*w*/*w*) PEG 8000, 0.1 *M* Tris–HCl pH 8.5, 0.2 *M* $MgCl_2$. Each drop contained 1.5 µl WbmG (16 mg ml^{-1}) and 1.5 µl mother liquor. Crystals grew rapidly and after 7 d good-quality crystals had reached dimensions of 50 × 30 × 30 µm (Fig. 1*b*). Similar crystals of selenomethionine-labelled WbmG grew under identical conditions.

One diffraction-quality crystal of WbmH was found in the initial sparse-matrix screen in Crystal Screen I, condition 41, using 5 mg ml^{-1} WbmH. The mother liquor contained 10%(*v*/*v*) 2-propanol, 20%(*w*/*v*) PEG 4000, 0.1 *M* HEPES pH 7.5. The crystal grew over 11 d and reached dimensions of 30 × 10 × 10 µm (Fig. 1*c*). Subsequent attempts to optimize this condition did not provide crystals of the same quality and this crystal proved sufficient to solve the structure to a good resolution.

Crystals of WbmF and WbmG were soaked with nucleotides or nucleotide sugars by preparing an artificial mother liquor containing 16%(*w*/*w*) PEG 8000, 0.1 *M* Bicine pH 9.0 (for WbmF) or 16%(*w*/*w*) PEG 8000, 0.1 *M* Tris–HCl pH 8.5, 0.2 *M* $MgCl_2$ (for WbmG) supplemented with 10 m*M* nucleotide or sugar nucleotide. Crystals were incubated in this mother liquor for 5–30 min and then transferred to cryocooling solution. The cryocooling solution used for WbmF crystals was 16%(*w*/*w*) PEG 8000, 0.1 *M* Bicine pH 9.0, 20%(*v*/*v*) PEG 400; for WbmG, 16%(*w*/*w*) PEG 8000, 0.1 *M* Tris–HCl pH 8.5, 20%(*v*/*v*) PEG 400 was used as the cryocooling solution. The crystals showed no sign of damage after incubation in this solution for 1 min. The WbmH crystal was transferred to a cryocooling solution consisting of 8.5% 2-propanol, 17%(*w*/*v*) PEG 4000, 15% glycerol, 0.085 *M* HEPES pH 7.5 before cooling in liquid nitrogen.

A second crystal form of WbmF was obtained by cocrystallizing WbmF with NAD^+ and 10 m*M* UDP. One diffraction-quality crystal was found in the initial sparse-matrix screen in SM1 screen condition 59, using 14 mg ml^{-1} WbmF. The mother liquor contained 20%(*w*/*v*) PEG 3000, 0.1 *M* Tris pH 7.0, 0.2 *M* calcium acetate. The crystal grew in 7 d and reached dimensions of 100 × 100 × 50 µm. Attempts to reproduce the crystal were unsuccessful and this crystal provided data to an excellent resolution. The crystal was transferred to a cryoprotectant solution consisting of 24%(*w*/*v*) PEG 3000, 80 m*M* Tris pH 7.0, 160 m*M* calcium chloride and 20%(*v*/*v*) glycerol.

A second crystal form was obtained by cocrystallizing WbmG with 10 m*M* UDP. Diffraction-quality crystals were optimized from Crystal Screen I condition 39. The mother liquor contained 1.6 *M* ammonium sulfate, 2%(*v*/*v*) PEG 400, 0.1 *M* HEPES pH 7.5, 10 m*M* UDP. Each drop contained 2 µl WbmG solution (16 mg ml^{-1}) and 2 µl mother liquor. Crystals grew in 11 d to dimensions of approximately 100 × 50 × 50 µm. Crystals were transferred to a cryocooling solution consisting of 1.6 *M* ammonium sulfate, 2%(*v*/*v*) PEG 400, 0.1 *M* HEPES pH 7.5, 15%(*v*/*v*) glycerol.

4. X-ray analysis

4.1. X-ray data collection of WbmF crystals

High-resolution data sets for WbmF crystals were obtained at 100 K at beamline ID14-4 at ESRF (Grenoble, France). Data were collected over 200° with 1° oscillation per image on an ADSC Quantum-315 detector (Fig. 2). One crystal (WbmF in complex with NADH) gave particularly strong diffraction and so a second data set covering the same oscillation range was collected using strong attenuation to ensure that a complete data set was collected at low resolution.

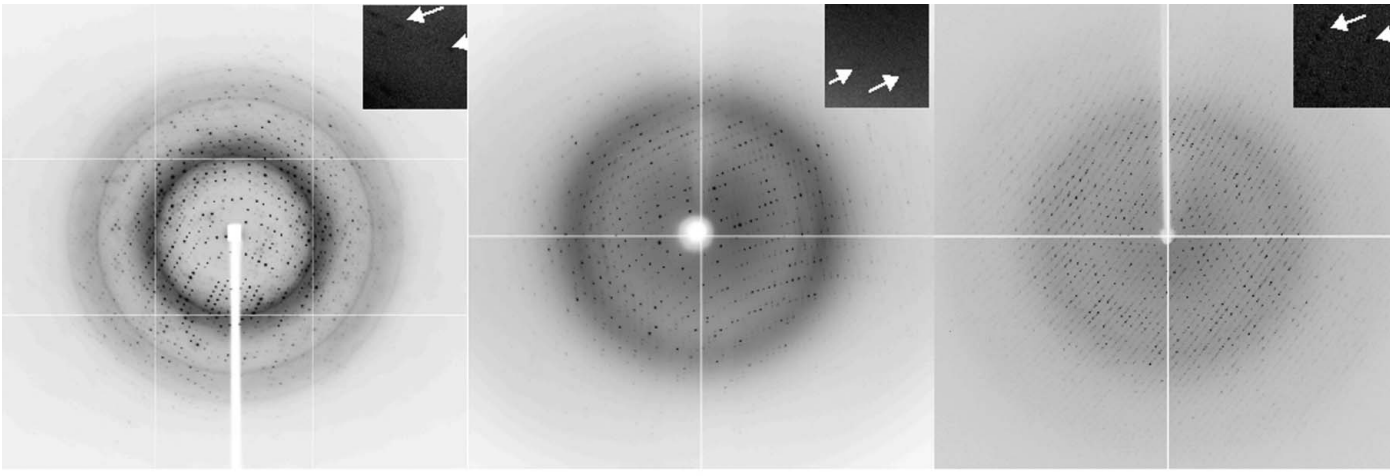

Figure 2
Representative images from the data collection for the apo forms of WbmF, WbmG (GDP-mannose soak) and WbmH are shown. Each image corresponds to the first image collected at the synchrotron source. Inset are closer views of the same image at the resolution edge, with the contrast reset to highlight visible spots at the edge, marked by arrows. (*a*) WbmF in complex with NADH; the arrowed spots both correspond to 1.50 Å. (*b*) WbmG soaked with GDP-mannose; the arrowed spots correspond to 2.10 Å (left) and 2.08 Å (right). (*c*) WbmH; the arrowed spots correspond to 2.20 Å (left) and 2.15 Å (right). The resolution edges after integration and scaling were chosen at 1.50, 2.10 and 2.20 Å, respectively.

Table 1
Data-collection statistics for native data sets.

Values in parentheses are for the highest resolution shell.

	WbmF–NAD$^+$	WbmF–NADH	WbmF–NAD$^+$–UDP soak	WbmF–NAD$^+$–UDP cocrystal	WbmG–GDP–Man soak	WbmG–UDP–Glc soak	WbmG–UDP cocrystal	WbmH
Space group	*C*2	*C*2	*C*2	*C*2	*C*2	*C*2	$C222_1$	$P2_12_12$
Unit-cell parameters								
a (Å)	82.88	83.19	83.44	121.85	192.04	191.23	58.21	93.67
b (Å)	77.88	77.86	78.12	79.68	49.76	49.79	140.48	158.99
c (Å)	59.23	59.41	59.26	84.95	76.02	75.91	184.14	68.22
α (°)	90	90	90	90	90	90	90	90
β (°)	108.17	108.19	108.08	113.10	101.13	101.12	90	90
γ (°)	90	90	90	90	90	90	90	90
Matthews coefficient (Å^3 Da^{-1})	2.16	2.17	2.16	2.23	2.49	2.45	2.60	2.28
Solvent content (%)	43.1	43.4	43.1	45.0	50.6	49.8	52.7	46.1
Unit-cell volume (Å^3)	363220	365646	367220	758697	712807	769223	1505882	1016022
Molecules per ASU	1	1	1	2	2	2	2	3
Molecules per unit cell	4	4	4	8	8	8	16	12
Unique reflections	27275	57271	33895	81311	38661	27549	51158	49975
Resolution range	50–1.90 (1.93–1.90)	50–1.5 (1.53–1.50)	50–1.75 (1.78–1.75)	50–1.7 (1.73–1.70)	30–2.1 (2.15–2.1)	30–2.4 (2.46–2.40)	30–2.0 (2.03–2.00)	30–2.2 (2.25–2.2)
Completeness (%)	96.6 (77.4)	99.3 (94.8)	93.3 (62.6)	98.4 (87.1)	97.6 (79.2)	98.7 (97.7)	99.9 (100)	93.9 (91.3)
Redundancy	4.6 (3.0)	4.8 (3.7)	3.9 (2.4)	3.9 (2.9)	3.83 (3.08)	4.47 (4.45)	5.9 (5.9)	5.22 (3.58)
$R_{\rm merge}$†	3.9 (22.3)	5.2 (65.8)	4.9 (33.7)	5.5 (45.9)	7.5 (48.3)	10.3 (32.8)	8.5 (77.3)	11.4 (38.0)
$\langle I/\sigma(I)\rangle$	32.1 (5.89)	29.5 (1.83)	23.7 (2.38)	21.9 (2.18)	16.9 (2.14)	15.0 (3.98)	19.6 (2.28)	15.2 (3.63)
Data-collection wavelength (Å)	0.977	0.977	0.977	0.977	1.488	1.488	0.977	0.9340/1.488
PDB code	2pzj	2q1s	2q1t	2q1u	2pzk	2pzl	2pzm	2q1w

† $R_{\rm merge} = \sum_{\mathbf{h}}\sum_i |I_{\mathbf{h}i} - \langle I_{\mathbf{h}}\rangle| / \sum_{\mathbf{h}}\sum_i \langle I_{\mathbf{h}}\rangle$, where I_i is the ith observation of reflection **h** and $\langle I_{\mathbf{h}}\rangle$ is the weighted average intensity for all observations l of reflection **h**.

4.2. X-ray data collection of WbmG crystals

High-resolution data sets from these crystals were obtained at 100 K. Data for WbmG soaked with GDP-mannose (Fig. 2), WbmG soaked with UDP-glucose and selenomethionine-labelled WbmG were collected at beamline PX14.2 at the Daresbury SRS (Daresbury, UK). Data were collected over 200° with 1° oscillation per image on an ADSC Quantum-100 detector, except for the MAD data, where data were collected at peak (720°), inflection (720°) and remote wavelengths (360°). Data for WbmG cocrystallized with UDP were collected at beamline ID14-4 at ESRF (Grenoble, France). Data were collected at 100 K over 110° with oscillations of 0.2–1° per image on an ADSC Quantum-100 detector. Appropriate oscillation angles for avoiding overlaps were determined using *MOSFLM* (Leslie, 1992).

4.3. X-ray data collection of the WbmH crystal

A high-resolution data set from this crystal was obtained at 100 K. Data were collected at station ID29 at ESRF (Grenoble, France). Data were collected over 90° with 0.5° oscillation per image on an ADSC Quantum-315 detector (Fig. 2). Subsequently, a low-resolution data set was collected at the Daresbury SRS (Daresbury, UK). Data were collected over 180° with 1° oscillation per image on an ADSC Quantum-100 detector.

4.4. Processing of X-ray data

The data were processed using *DENZO* and scaled using *SCALEPACK* (Otwinowski & Minor, 1997). The space groups determined, the unit-cell parameters and the crystallographic data are summarized in Table 1. Based on the packing densities (Matthews, 1968; Collaborative Computational Project, Number 4, 1994) and solvent contents of the crystals with the expected number of protein molecules in the asymmetric unit (full details in Table 1), WbmF is likely to have one molecule per asymmetric unit. The crystal form obtained for cocrystals of WbmF with UDP is likely to have two molecules per asymmetric unit, as this leads to a packing density almost identical to that of the previous crystal form. For WbmG in the *C*2 crystal form, two monomers per asymmetric unit are the most likely. The $C222_1$ crystal form also has an acceptable packing density with two monomers in the asymmetric unit. For WbmH, it is most likely that the unit cell contains three monomers per asymmetric unit; however, either two or four monomers per asymmetric unit would correspond to precedented values for the packing density and solvent content.

Three previously solved protein structures have similar homology to WbmF (PDB codes 1bxk, 1keu and 1r6d). Each of these proteins has 26–27% sequence identity to WbmF. These three proteins, with nonhomologous side chains truncated to C$^\gamma$, were used as molecular-replacement probes. Molecular replacement using *Phaser* (McCoy *et al.*, 2005) and *MOLREP* (Vagin & Teplyakov, 1997) gave identical solutions. Following density modification with *DM* (Cowtan, 1994), the electron density became interpretable and permitted structure solution. The refined structure of WbmF (King *et al.*, 2007) was used as a molecular-replacement probe for the second crystal form. Molecular replacement using *Phaser*, with a crystallographic dimer of WbmF as the model, provided a successful solution.

Although there is a previously solved structure of a homologue of WbmG with a sequence identity of 28% (PDB code 1r66), molecular replacement proved unsuccessful; solutions with seemingly excellent correlations to the data could not be refined (data not shown). A self-rotation function was calculated for the *C*2 crystal form and this revealed that there was a noncrystallographic twofold rotation axis between the two molecules in the asymmetric unit, which was closely aligned with the crystallographic twofold rotation axis. It seemed likely that the alignment of the two axes made molecular replacement impossible. Therefore, we prepared selenomethionine-labelled protein and obtained diffraction data from labelled WbmG (Table 2). Analysis of this data using *SOLVE* (Terwilliger & Berendzen, 1999) demonstrated that eight of the ten potential selenium sites could be convincingly found at full occupancy, indicating that the structure could be solved from this data.

Following the solution of the structure of WbmG, structure solution of WbmH using molecular replacement was attempted. WbmG shows 40% sequence identity to WbmH, whereas no other protein

Table 2
Data-collection statistics for WbmG MAD data.

Values in parentheses are for the highest resolution shell.

	Peak	Inflection	Remote
Space group	*C*2		
Unit-cell parameters	a = 190.86, b = 48.91, c = 75.77, α = 90, β = 101.0, γ = 90		
Wavelength	0.97905	0.97938	0.97668
Resolution (Å)	30–2.65 (2.71–2.65)	30–2.65 (2.71–2.65)	30–2.65 (2.71–2.65)
$R_{\rm merge}$†	6.9 (24.0)	7.3 (28.9)	7.0 (24.7)
$\langle I/\sigma(I)\rangle$	41.0 (12.1)	40.4 (10.5)	27.9 (8.47)
Completeness (%)	100 (100)	100 (100)	100 (100)
Redundancy	14.5 (14.8)	14.5 (14.8)	7.27 (6.96)

† $R_{\rm merge} = \sum_{\mathbf{h}}\sum_{l}|I_{\mathbf{h}l} - \langle I_{\mathbf{h}}\rangle|/\sum_{\mathbf{h}}\sum_{l}\langle I_{\mathbf{h}}\rangle$, where I_l is the lth observation of reflection **h** and $\langle I_{\mathbf{h}}\rangle$ is the weighted average intensity for all observations l of reflection **h**.

with a solved structure has a sequence identity to WbmH of above 22%. However, attempts to find a solution to the molecular-replacement problem using *Phaser*, *MOLREP* or *AMoRe* (Navaza, 1994) were unsuccessful using the high-resolution data set. Examination of the data suggested that the low completeness of the data, particularly in the lowest resolution shell (completeness only 83%), might be the cause of the failure to determine the solution. Therefore, a second data set was collected with a focus on ensuring 100% completeness in all resolution shells. The crystal showed significant radiation damage from the collection of the first data set and therefore the quality and resolution of the data were considerably poorer than for the first data set. However, with this complete data set *Phaser* was able to determine the correct molecular-replacement solution, with three molecules in the asymmetric unit. By scaling the two data sets together, a satisfactory data set with more accurate data and a higher completeness in the lower resolution shells (>95%) was obtained and the electron density was clearly interpretable following molecular replacement.

A full description of the refinement of these structures and their implications will be reported elsewhere (King *et al.*, 2007).

References

Burns, E. H. Jr, Norman, J. M., Hatcher, M. D. & Bemis, D. A. (1993). *J. Clin. Microbiol.* **31**, 1838–1844.
Burns, V. C., Pishko, E. J., Preston, A., Maskell, D. J. & Harvill, E. T. (2003). *Infect. Immun.* **71**, 86–94.
Cherry, J. D. (1996). *J. Infect. Dis.* **174**, *Suppl.* 3, S259–S263.
Collaborative Computational Project, Number 4 (1994). *Acta Cryst.* D**50**, 760–763.
Cowtan, K. (1994). *Jnt CCP4/ESF–EACBM Newsl. Protein Crystallogr.* **31**, 34–38.
Ginsburg, V. (1960). *J. Biol. Chem.* **235**, 2196–2201.
Ginsburg, V. (1961). *J. Biol. Chem.* **236**, 2389–2393.
Giraud, M. F. & Naismith, J. H. (2000). *Curr. Opin. Struct. Biol.* **10**, 687–696.
King, J. D., Harmer, N. J., Preston, A., Palmer, C. M., Rejzek, M., Field, R. A., Blundell, T. L. & Maskell, D. J. (2007). Submitted.
Leslie, A. G. W. (1992). *Jnt CCP4/ESF–EACBM Newsl. Protein Crystallogr.* **26**.
McCoy, A. J., Grosse-Kunstleve, R. W., Storoni, L. C. & Read, R. J. (2005). *Acta Cryst.* D**61**, 458–461.
Magyar, T., Chanter, N., Lax, A. J., Rutter, J. M. & Hall, G. A. (1988). *Vet. Microbiol.* **18**, 135–146.
Major, L. L., Wolucka, B. A. & Naismith, J. H. (2005). *J. Am. Chem. Soc.* **127**, 18309–18320.
Matthews, B. W. (1968). *J. Mol. Biol.* **33**, 491–497.
Navaza, J. (1994). *Acta Cryst.* A**50**, 157–163.
Otwinowski, Z. & Minor, W. (1997). *Methods Enzymol.* **276**, 307–326.
Porter, J. F., Connor, K. & Donachie, W. (1994). *Microbiology*, **140**, 255–261.
Preston, A., Allen, A. G., Cadisch, J., Thomas, R., Stevens, K., Churcher, C. M., Badcock, K. L., Parkhill, J., Barrell, B. & Maskell, D. J. (1999). *Infect. Immun.* **67**, 3763–3767.
Terwilliger, T. C. & Berendzen, J. (1999). *Acta Cryst.* D**55**, 849–861.
Tonetti, M., Sturla, L., Bisso, A., Zanardi, D., Benatti, U. & De Flora, A. (1998). *Biochimie*, **80**, 923–931.
Vagin, A. & Teplyakov, A. (1997). *J. Appl. Cryst.* **30**, 1022–1025.
Van Duyne, G. D., Standaert, R. F., Karplus, P. A., Schreiber, S. L. & Clardy, J. (1993). *J. Mol. Biol.* **229**, 105–124.